Intensive Care Med (2003) 29:111–118
DOI 10.1007/s00134-002-1547-4

EXPERIMENTAL

**Nathalie Bernard**
**Stefan Matecki**
**Guillaume Py**
**Sandrine Lopez**
**Jacques Mercier**
**Xavier Capdevila**

# Effects of prolonged mechanical ventilation on respiratory muscle ultrastructure and mitochondrial respiration in rabbits

Received: 10 January 2002
Accepted: 4 October 2002
Published online: 20 November 2002


N. Bernard · S. Lopez · X. Capdevila (✉)
Département d'Anesthésie Réanimation A,
Hôpital Lapeyronie and UPRES EA 701,
371 avenue du Doyen Giraud,
34295 Montpellier, France
e-mail: x-capdevila@chu-montpellier.fr
Tel.: +33-4-67338256
Fax: +33-4-67337960

S. Matecki · G. Py · J. Mercier
Laboratoire de Physiologie des Interactions
and UPRES EA 701,
Hôpital Arnaud de Villeneuve,
371 avenue du Doyen Giraud,
34295 Montpellier, France

**Abstract** *Objective:* To investigate in rabbits whether prolonged mechanical ventilation (PMV) leads to ultrastructural changes in respiratory muscles and alters diaphragm mitochondrial respiration. *Design and setting:* Experimental prospective study in a university laboratory. *Animals and interventions:* We studied respiratory muscles of seven rabbits after 49±1 h of controlled mechanical ventilation. Ten non-ventilated rabbits were used as a control group. *Measurements and results:* After mechanical ventilation electron-microscopic observations of the diaphragm and the external intercostal muscles revealed disrupted myofibrils, increased number of lipid vacuoles in the sarcoplasm, and smaller mitochondria with focal membrane disruptions. Volumetric and numerical densities of the mitochondria were significantly lower in the PMV group than the control group. Mitochondrial respiration was quantified in isolated diaphragm muscle-cell mitochondria using two respiratory substrates. There was no difference in oxygen consumption values in the three states of mitochondrial respiration between the two groups except for state 2 (basal state) with pyruvate/malate parameter (53.5±20 for the ventilated group vs. 33.8±10.2 nmol atom O/mg per minute for the control group). There was no significant difference between groups in ADP/O ratio or respiratory control ratio. *Conclusions:* PMV leads to respiratory muscle cell degeneration and minor changes in oxidative phosphorylation coupling in diaphragmatic mitochondria. These phenomena may mediate part of damage of respiratory muscles after inactivity related to PMV.

**Keywords** Oxidative phosphorylation · Disuse · Diaphragm · Weaning

## Introduction

Mechanical ventilation (MV) is widely used to manage respiratory failure [1]. During controlled MV respiratory muscle activity stops, as demonstrated by the absence of diaphragmatic electrical activity [2]. The contribution of respiratory muscles weakness to respiratory failure, and the possible causative role of muscle inactivity in contributing to this weakness, remains unknown [3, 4, 5, 6]. Many skeletal muscle changes have been found after immobilization, hypokinesia, or denervation. These changes include atrophy [7], alterations in contractile properties with decrease in fatigue resistance indexes [8, 9], alterations in mitochondrial respiration, affecting primarily complex 1 of the electron transport chain [10, 11, 12, 13], and modifications in muscle cell ultrastructure [14, 15, 16]. In the same way diaphragmatic disuse caused by denervation, cervical spinal cord isolation, and tetrodotoxin blockade of nerve impulses have been shown to affect contractile and morphometric properties, endurance capacities [2, 17, 18, 19, 20], and ultrastructural morphology [17, 21].

Only limited information is available concerning the effects of respiratory muscle disuse caused by prolonged MV (PMV). Le Bourdelles et al. [22] reported that MV for 48 h in rats was correlated with decreased muscle weight and altered in vitro contractile properties of the diaphragm. Anzueto et al. [23] demonstrated that MV for 11 days resulted in decreased diaphragm muscle strength and endurance in baboons. Modifications in myosin heavy chain distribution have also been reported in rats after 3–7 days of MV [24]. To our knowledge, there are no reports in the literature directly concerning the effects of PMV on the oxidative capacities of respiratory muscles. Muscle endurance is known to be dependent on mitochondrial activity [25], and oxidative capacities are highly altered in skeletal muscle disuse. Furthermore, mitochondria seems to be the main target of cellular damages and partially mediates mechanisms which lead to cellular apoptosis [26]. Similarly, we found no studies of ultrastructural repercussions of PMV on muscle cells, even though substantial ultrastructural modifications have been shown after diaphragm denervation [17, 21] or skeletal muscle immobilization [14, 15, 16]. We hypothesized that inactivity induced by PMV has a detrimental effect on respiratory muscle ultrastructure and mitochondrial respiration.

The purpose of this study conducted on rabbits was to evaluate the impact of MV for 48 h on both electron-microscopic ultrastructure of respiratory muscle cells and respiration of mitochondria isolated from the diaphragm.

## Materials and methods

### Experimental model

We developed an original model of PMV in rabbits. Care of the animals conformed to the recommendations of the institutional Animal Care Committee and the French Ministry of Agriculture. Seventeen adult New Zealand rabbits (INRA, Montpellier, France) were studied. Following overnight fasting to empty the stomach the animals were randomly divided into two groups, a PMV group ($n$=7) and a control group ($n$=10). PMV rabbits were ventilated for 49±1 h. They remained afebrile with body temperature ranging from 37° to 38.5°C, urinated spontaneously, and maintained gastrointestinal transit throughout the study. No significant difference was noted between PMV and control rabbits in terms of weight before experimentation (3236±585 g in the PMV group vs. 2911±192 g in the control group, $p$=0.34).

PMV rabbits were premedicated with intramuscular ketamine (50 mg/kg), diazepam (2.5 mg/kg), and atropine (0.125 mg) [27]. They were tracheotomized after local (2% subcutaneous lidocaine, Astra-Zaneca, France) and general anesthesia (7.5 mg/kg intravenous ketamine) and mechanically ventilated for more than 48 h using a volume-cycled ventilator (RP 200, Fontenay-sous-bois, France) with 50% $FIO_2$, tidal volume at 8 ml/kg, respiratory rate at 60/min, ratio of inspiratory time to total respiratory time at 1/1.5, and a positive end-expiratory pressure of 2 $cmH_2O$. During MV an intravenous femoral catheter was used for both anesthesia by continuous infusion of sodium thiopental (15 mg/kg per hour), and continuous parenteral nutrition with a nutrient composition of 60% carbohydrate, 25% lipids, 15% proteins, vitamins and minerals (100 ml/kg per 24 hour, corresponding to 42 kcal/kg per day). To prevent infection and thromboembolic events cefamandole (50 mg/kg) and heparin (2 mg/kg per 24 hour) were administered intravenously. Neuromuscular blocking agents were not used. The animal's temperature was recorded and maintained at 38°C by an electric blanket. Four needle electrodes were subcutaneously implanted in the abdomen and connected to a cardioscope (E1 130, Philips, Amsterdam, The Netherlands) allowing continuous electrocardiographic and heart rate measurements. The control group animals were anesthetized according to the same protocol and ventilated for 30 min using the same parameters previously described for the PMV group. At the end of the MV period in each group a costal portion of the diaphragm and the 5th and 6th external intercostal muscles were removed through a laparotomy before killing the animal by exsanguination.

### Electron microscopy

A costal portion of the diaphragm (2×2 mm) and the 5th and 6th external intercostal muscles were excised and quickly placed in 2.5% glutaraldehyde in 0.2 M phosphate-buffered saline at room temperature for 2 h. The samples were then rinsed three times in cacodylate buffer (pH=7.4), 10 min per rinse and postfixed in 1% buffered osmium tetroxide, dehydrated in a graded alcohol series, immersed in 100% propylene oxide, and embedded in Spurr's resin (Epon). Thin 70-nm longitudinal sections from the samples were cut using an ultramicrotome and stained with lead citrate and uranyl citrate. Four rabbits randomly chosen in both groups were studied, and in an effort to avoid inadequate sampling four pieces of each kind of muscle (diaphragm and intercostal muscles) were examined per animal. The sections were examined in a transmission electron microscope (Hitachi H 7100, Japan), and photomicrographs were taken.

The morphometric analysis was performed at a magnification of ×15,000. The sections were studied on a grid of square elements to permit counting the total number of points per cell section (*tp*), the number of points included on the mitochondria area (*mp*), or on the myofibrils (*mfp*) and the number of mitochondrial sections per cell slice (*mn*). These parameters permit determination of the volumetric density (*Vd*) and numeric density (*Nd*) of the mitochondria and myofibrils:

*VD* mito=*mp*/*tp* *Nd* mito=*mn*/*tp* *Vd* myof=*mfp*/*tp*

### Whole muscle mitochondrial isolation

The muscle sample was immediately placed in ice-cold isolation medium (IM) containing 250 mM mannitol, 10 mM EDTA, 45 mM Tris-HCl, and 5 mM Tris base, pH 7.4 at 4°C [25]. The mitochondria were isolated from the costal diaphragm according to the method described by Davies et al. [25]. The diaphragm was free of fat and connective tissue, transferred into fresh IM, and weighed. All further procedures were carried out between 0° and 5°C. The diaphragm sample was next minced with triple scissors in a 1:9 dilution of fresh IM, and homogenized with a Thomas tissue homogenizer (Poly Labo, Strasbourg, France) using four slow passes of the pestle. A first centrifugation at 500 *g* (Jouan, model KR 4.22, Saint-Herblain, France) for 10 min separated the mitochondria. The homogenate was then centrifuged twice (8000 *g*) for 10 min each time and the final mitochondrial pellets were suspended in 1 ml IM. Mitochondria were kept on ice until mitochondria respiration measurements were performed. The final mitochondria protein concentration was determined using a Bradford protein assay (Bio-Rad) with bovine serum albumin as standard [28].

### Mitochondrial respiration study

Mitochondrial oxygen consumption measurements were determined using a complete oxygen measurement system consisting of

an oxygen meter (Strathkelvin system, model 781), a microcathode oxygen electrode (Clark type polarographic electrode), and a respiration chamber (3 ml) set at 37°C. When the electrode was assembled, it was calibrated, the zero value being obtained with a sodium borate solution (2.0 ml of a 0.01 M solution) added to the chamber with crystals of sodium sulfite. The maximal value was calibrated with respiration medium alone (1.87 ml) containing 15 mM KCl, 30 mM $K_2HPO_4$, 25 mM Tris base, 45 mM sucrose, 12 mM mannitol, 5 mM $MgCl_2$, 7 mM EDTA, 0.2% bovine serum albumin, and 20 mM glucose, pH 7.4; this value corresponded to 780.0 mol atomic oxygen. One of the two substrates was added to the respiration chamber: 10 mM pyruvate and 2.5 mM malate, or 10 mM succinate with 5.0 µM rotenone added to inhibit complex 1 (NADH reductase) of the electron transport chain. A capillary-shaped opening in the electrode allowed sequential addition of substrate with no risk of air diffusing into the chamber. Then 1 mg of isolated mitochondria was loaded into the chamber with a magnetic stirring apparatus to ensure complete mixing of mitochondria and substrate. ADP at 250 µM final concentration was added to initiate state 3 of mitochondrial respiration (ADP-stimulated). State 4 was defined as oxygen consumption of mitochondria after the depletion of exogenous ADP. The respiratory control ratio (RCR) was obtained by dividing state 3 respiration by the recovery rate in state 4. Oxygen consumption was determined as the amount of oxygen disappearing from the respiration chamber over time per 1 mg mitochondrial protein. The ADP/O ratio was calculated, corresponding to the amount of ADP phosphorylated to ATP divided by the oxygen consumed during state 3 respiration [29].

### Statistical analysis

Statistical analysis was performed using SigmaStat statistical software (Jandel, Chicago, Ill., USA). Data are reported as mean values ±SEM or median and 10, 25, 75 and 90th percentiles. Significance of differences in mean values for animal weight, MV duration, and mitochondrial respiration data between the two groups were assessed by Student's paired *t* test and by the Mann-Whitney nonparametric test as appropriate. A *p* value of 0.05 was taken as indicating statistical significance.

## Results

### Ultrastructural study

Electron-microscopic observations revealed evidence of altered ultrastructure indicative of fiber injury in the PMV group muscles but not in the control group muscles.

#### *Respiratory muscles of control rabbits*

The control group rabbit respiratory muscles showed normal myofibrillar ultrastructure, with Z, I, A and M bands (composed of thin and thick myofilaments; Fig. 1a, c). The myofibrils were separated by small bands of sarcoplasm (Fig. 1a) containing normal mitochondria with evenly arranged cristae and narrow matrix spaces between cristae, sarcoplasmic reticulum, glycogen, lipids, and ribosomes (Fig. 1b). There were no ultrastructural abnormalities in the control muscles. In particular, there were no anomalies of mitochondrial morphology, indicating that the handling and preparation procedures for the muscle samples did not induce morphological artifacts.

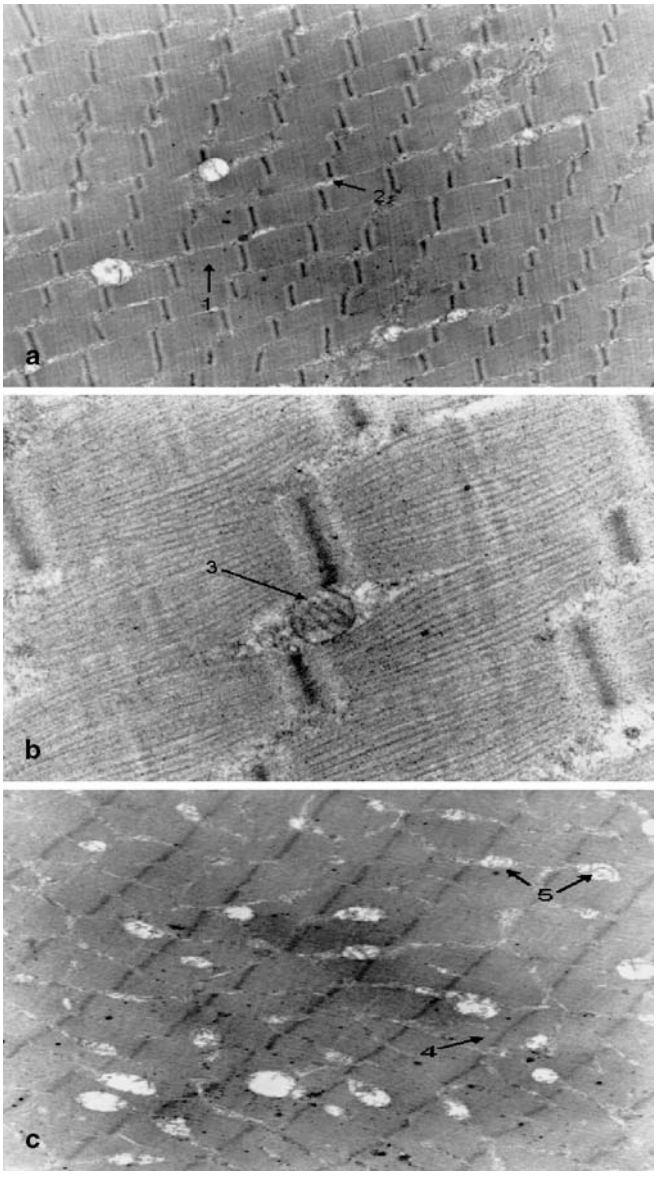


**Fig. 1a–c** Control rabbit respiratory muscle ultrastructure. Longitudinal sections. **a** Diaphragm control rabbit, ×6,000. Normal ultrastructure of myofibrils. *1* Normal sarcomeric structure; *2* small band of sarcoplasm. **b** Diaphragm of control rabbit, ×30,000. *3* The mitochondrial architecture is normal. **c** External intercostal muscles of a control rabbit, ×6,000; *4* normal myofibrillar ultrastructure; *5* normal mitochondria

#### *Costal diaphragm of ventilated animals*

After 49±1 h of MV we observed disruption and fragmentation of myofibrils, which consisted of normal

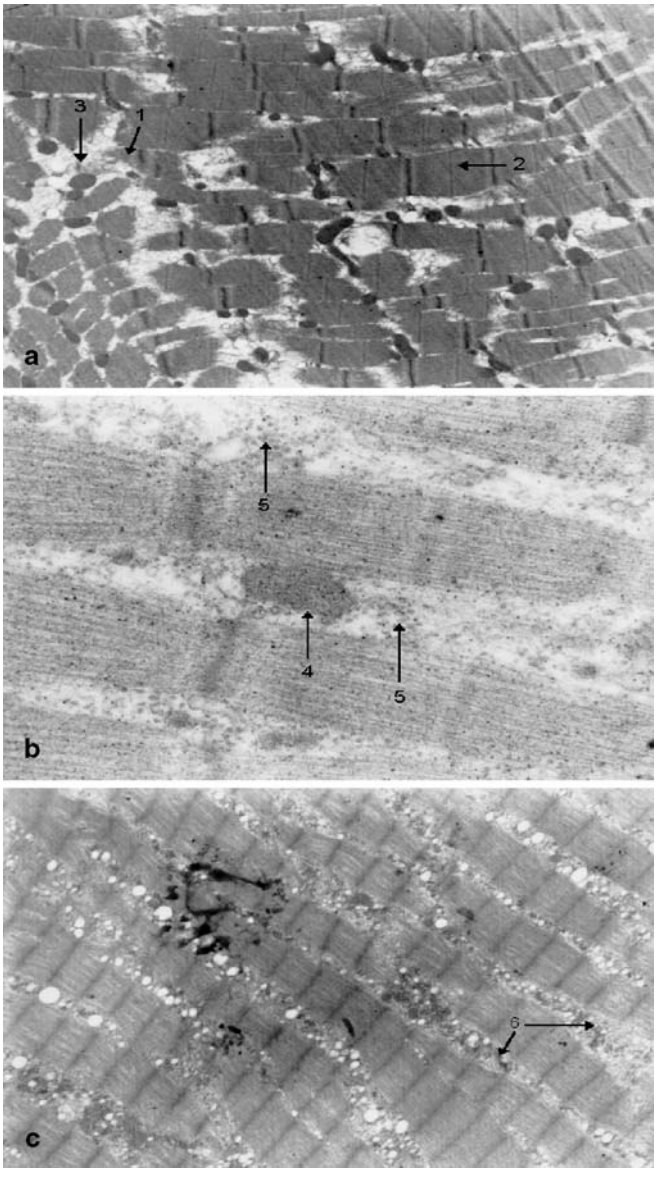


**Fig. 2a–c** Ventilated rabbit respiratory muscle ultrastructure. Longitudinal sections. **a** Diaphragm of ventilated rabbit, ×6,000. Disruption and fragmentation of myofibrils, with large interfibrillar space. *1* Disintegrated sarcomere; *2* preserved sarcomere; *3* sarcoplasmic disorganization. **b** Diaphragm-ventilated rabbit, ×40,000. *4* Smaller mitochondria, disruption of outer membranes; *5* increase in sarcoplasmic granular material and cytoplasmic lipid vacuoles. **c** External intercostal muscle of ventilated rabbit. ×6,000; *6* increase in sarcoplasm lipid vacuoles and in connective tissue

sarcomeric structure containing well preserved myofilaments adjacent to sarcomeres in various stages of disintegration. The fibers exhibited a normal arrangement of contractile filaments and Z-line pattern, even though the myofibrils were fragmented. Z bands, thick A-band, and thin I-band myofilaments remained unchanged (Fig. 2a). However, we observed a large interfibrillar space containing increased amounts of granular material, cisternae with glycogen and many sarcoplasmic vacuoles probably corresponding in part to degenerated triads of sarcoplasmic reticulum (Fig. 2b). There were fewer mitochondria and they were smaller and less regularly arranged than control diaphragms. They were located next to the Z-bands. They were very electron dense, as was the case in the control diaphragms. At higher magnification (×40,000) the mitochondrial external membrane appeared disrupted and the internal cristae blurred, perhaps beginning to disintegrate (Fig. 2b). We did not observe vacuolated or swollen mitochondria.

*External intercostal muscles of ventilated rabbits*

Fragmentation of myofibrils with disrupted sarcomeres was observed. There was a substantial increase in the number and size of sarcoplasmic lipid vacuoles and connective tissue, with large irregularly shaped areas of disorganized sarcoplasm. Mitochondrial outer membranes were in part disrupted (Fig. 2c).

## Morphometric study

Morphometric analysis of the diaphragm showed that the volumetric density of the mitochondria was lower in the PMV group than in the control group (0.219± 0.07 and 0.410±0.03 respectively, $p$=0.02) and also the numerical density (0.082±0.03 and 0.168±0.02 respectively, $p$=0.05). The volumetric density of the myofibrils did not differ significantly between the two groups (0.807±0.05 vs. 0.861±0.08 in the control group, $p$=0.42).

## Mitochondrial respiration study

For both substrates Table 1 reports the values of mitochondrial oxygen consumption for each state in both groups. With pyruvate/malate there was no significant difference between the control and the PMV groups for oxygen consumption values in states 3 and 4. However, state 2 values were significantly higher ($p$=0.01) in the PMV group than in the control group. With succinate/rotenone as respiratory substrate, despite a tendency toward an increase in respiratory rate, no significant difference in mitochondrial respiration rates were found between groups for the three states. No statistically significant difference was found for either respiratory substrate regarding ADP/O ratio and RCR (Table 2).

**Table 1** Oxygen consumption in the three states in the prolonged mechanical ventilation group (*PMV*) and controls; oxygen consumption (nmol atom O/mg per minute) with the two respiratory substrates. Median (*Med*) and interquartile (*IQ*) range

| | Pyruvate-malate | | | | Succinate-rotenone | | | |
|---|---|---|---|---|---|---|---|---|
| | PMV | | Control | | PMV | | Control | |
| | Med | IQ range | Med | IQ range | Med | IQ range | Med | IQ range |
| Basal state | 46* | 37.5–69.3 | 33.6 | 27.3–42 | 105.9 | 90.5–220.7 | 113.5 | 84.3–129.5 |
| ADP-stimulated state | 221 | 184.8–409.8 | 207.4 | 190.7–258 | 238.2 | 163.8–594.3 | 259 | 198.6–282.7 |
| Recovery state | 56.5 | 36.1–91 | 51.4 | 31.8–61 | 118.2 | 100.1–231.7 | 137.9 | 117.2–166.7 |

* $p<0.05$ vs. control

**Table 2** Phosphorylated/oxygen consumed ratio (*ADP/O*) and respiratory control ratio (*RCR*) values in prolonged mechanical ventilation group (*PMV*) and controls with both respiratory substrates. Median (*Med*) and interquartile (*IQ*) range

| | Pyruvate-malate | | | | Succinate-rotenone | | | |
|---|---|---|---|---|---|---|---|---|
| | PMV | | Control | | PMV | | Control | |
| | Med | IQ range | Med | IQ range | Med | IQ range | Med | IQ range |
| ADP/O | 2.8 | 2.2–3.2 | 3.2 | 3.1–3.3 | 1.5 | 1.4–1.8 | 1.6 | 1.4–1.7 |
| RCR | 4.8 | 3.4–5.1 | 4.4 | 4–4.7 | 2.1 | 1.9–2.3 | 1.9 | 1.6–2.1 |

## Discussion

The main findings of this study are that 49±1 h of MV led to disruption of respiratory muscle myofibrils and to an increase in the size of the interfibrillar space and in the number and size of sarcoplasmic lipid vacuoles. Smaller mitochondria with focal disruption of their outer membrane were also observed in respiratory muscle cells, confirmed by the lower numerical and volumetric densities. Concerning diaphragm mitochondrial oxygen consumption, only the basal state with pyruvate/malate as respiratory substrate was significantly increased. No significant difference in ADP/O ratio or RCR with either respiratory substrate was found after MV.

One-week immobilization models in rabbits have shown evidence of myofibril alterations with large irregularly shaped areas of disorganized sarcoplasm, multifocal loss of cross-striations, breaking-up of Z-bands, and an increase in the number and size of sarcoplasmic lipid vacuoles, granular material, and connective tissue in skeletal muscles [14, 15, 30, 31, 32, 33]. Regarding mitochondria, as little as 10 h of immobilization has been shown to lead to cystlike structures in the cristae and to reduced density, rounding, and slight swelling of mitochondria. Few studies have focused on ultrastructural modifications after diaphragm disuse. Miledi and Slater [34] conducted an electron-microscopic study of the mitochondria in normal and denervated rat hemidiaphragms. Less than 24 h after denervation the mitochondria were found to be smaller and less regularly arranged, with small circular shapes. At 72 h after diaphragm denervation alterations in Z-line and sarcomeric structure, cellular infiltration, and segmental fiber necrosis have been found [22]. Satellite cell mitotic activity was 5.5 times greater in denervated diaphragm than intact diaphragm. The authors concluded that acute unilateral diaphragm denervation by phrenic transection resulted in muscle fiber injury that induced satellite cell activation. In accordance with these previous studies, we found disruption of myofibrils, with preserved areas adjacent to disintegrated sarcomers [15, 30, 31, 33] and increased amounts of lipid vacuoles, glycogen granules, and connective tissue [14, 15, 31, 33]. As in the denervation studies, we observed changes in triads and sarcoplasmic reticulum [33, 35]. Concerning mitochondria, we did not observe swelling or alterations in cristae and matrix [14, 15, 32] but only smaller rounded mitochondria, which were irregularly located near the Z-bands. Alterations concerning cristae and matrix have previously been observed between 10 and 36 h after immobilization. Such changes may have disappeared by 48 h [15]. Our electron-microscopic observations were made at 48 h and the consistent differences between the muscles of the two rabbit groups processed under identical conditions attest to the validity of the results.

The present diaphragm muscle inactivity model using PMV differed from previous models of diaphragmatic inactivation. In denervation models communication between motoneurons and muscle is completely abolished. Furthermore, in the latter models there is passive stretching and consequent mechanical loading imposed on the denervated muscle fibers by the increased inspiratory

motion of the intact, contralateral side of the diaphragm [20]. Fiber-type disuse adaptations involve the action of transported neurotrophic substances and synthesized myotrophic factors. When using PMV models the communication between motoneurons and muscles persists while both are inactivated. The matched motoneuron and muscle activity may influence the adaptive response to disuse [19, 20]. Disuse of muscle after immobilization leads to focal autophagic activity of muscle cells. The mechanisms that initiate muscle degeneration are still unknown. Altered blood supply caused by immobility, variations in tension in different fibers, and lack of afferent stimuli in reflex arcs could be factors [32]. The myofibril fragmentation that we observed was similar to that reported in muscle injuries after anomalous contractions in human muscular dystrophy or in passive stretching [32]. The authors of the latter study hypothesized that as contractile elements disappear, massive production of energy is no longer necessary, and the mitochondria degenerate [32, 35]. The dilated and fragmented sarcoplasmic reticulum found in a variety of disorders also reflects the morphological disintegration that accompanies loss of function.

Despite the fact that the isolation procedure used in this study allowed us to obtain mitochondrial oxidation well coupled with ADP phosphorylation, as shown by the high RCR values, our results showed marked differences with those obtained by other authors after skeletal muscle immobilization. In studies of rat gastrocnemius muscles Max [12] showed that the ADP/O ratio and RCR decreased markedly from 1 to 6 days after skeletal fixation, indicating decreased phosphorylation efficiency. A significant decrease in state 3 respiration rate and RCR was observed in rats by Krieger et al. [11] after 2 days of hindlimb immobilization, Yajid et al. [13] after 4 weeks of hindlimb suspension, and Joffe et al. [10] using denervated rat soleus muscles. However, the mitochondria in the latter study displayed significantly higher state 4 respiratory rates than controls [10]. This implies that these mitochondria had poorly coupled oxidation and phosphorylation processes. No mitochondrial respiration measurements have been performed in respiratory muscles after immobilization or disuse. Diaphragm is not comparable to skeletal muscle. Its daily duty cycle ranges from 40% to 45% with continuous, repetitive activation [22], in contrast with the soleus and extensor digitorum longus muscles, having duty cycles of 14% and 2%, respectively [17]. The diaphragm may be particularly susceptible to disuse. In our study the significant increase in oxygen consumption in state 2 as measured by pyruvate/malate and the tendency to increase in states 3 and 4 could be explained by alterations in mitochondrial oxidative phosphorylation coupling [36]. According to the chemiosmotic theory, the driving force for mitochondrial ATP synthesis is the proton-motive force across the inner mitochondrial membrane, which is developed at the expense of electron transport and oxygen consumption. Inner membrane integrity allows protons to reenter the mitochondrial matrix only at sites where reentry is coupled to ATP synthesis, the F0F1-ATP synthase complex. Our results showed that mitochrondria after PMV have morphometric and ultrastructural alterations which could lead to functional abnormalities. We hypothesized that PMV compromises the permselectivity of the inner mitochondrial membrane permitting protons to leak back at nonspecific sites [36]. This phenomenon would increase oxygen consumption in the three states and decrease the efficiency of coupling from oxygen consumption to ATP production. We did not observe a decrease in the ADP/O ratio which would have confirmed this hypothesis. However, with pyruvate/malate as respiratory substrate the decreased ADP/O ratio values in the PMV group nearly reached significance ($p$=0.07).

We cannot exclude an effect of sodium thiopental. Several authors have shown that in vitro barbiturates inhibit mitochondrial electron transport and energy transfer and exert rotenonelike action (by inhibiting electron transport in the area of nicotinamide adenine nucleotide dehydrogenase) [37, 38, 39]. However, spectrophotometric studies have localized the site of action at several other parts of the electron transport chain [40]. The authors of various studies have concluded that barbiturates lead to in vitro uncoupling of oxidation and phosphorylation [37, 40, 41, 42]. In vitro studies of isolated liver or brain mitochondria have been reported in which the mitochondria were exposed directly at low temperatures [40] to high concentrations of barbiturates (largely exceeding those required to produce clinical anesthesia) [39]. Takaki et al. [43] investigated the respiratory function of mitochondria isolated from hearts of anesthetized rats with two different high doses of sodium pentobarbital (50 and 100 mg/kg). Respiratory function and electron transport were not suppressed in the isolated myocardial mitochondria of rat hearts after high-dose pentobarbital anesthesia, although the sodium pentobarbital blood concentration was of the same order as that which exerts mitochondrial uncoupling in rat isolated mitochondrial preparations. The authors concluded that sodium pentobarbital anesthesia up to 100 mg/kg is applicable for mechanoenergetic studies. Other variables could have caused the observed alterations. Prolonged anesthesia over 48 h can induce hemodynamic effects that may impair diaphragmatic blood flow. Acidosis or hypoxia may cause diaphragm ultrastructure changes. In a previous study we measured blood gases and hemodynamic parameters in nine ventilated rabbits (for 51±3 h, with the same ventilatory parameters as our study) and in ten control rabbits (ventilated for 30 min). We found no significant difference at the end of the ventilatory period between the two groups, concerning heart rate, systolic blood pressure, oxygen arterial pressure, carbonic gas arterial pressure, or pH.

When cells are subjected to aggression, mitochondria react in a limited stereotypical manner by a change in the conformation of mitochondrial proteins permitting entry of water from the matrix into the intermembrane space [44]. This early phase of mitochondrial contraction corresponds to the smaller and denser mitochondria observed after PMV. If the aggressive conditions persist, changes in the internal membrane appear and culminate in swelling of the mitochondria and clearing of the matrix, which can begin as early as the 10th h [14, 15]. The coupling of the flux of electrons to the synthesis of ATP depends more on the stability of the energetic state of the mitochondrial cristae membranes than on the integrity of the external membrane [45].

In conclusion, cell ultrastructural changes indicate respiratory muscle degeneration caused by muscular inactivity during MV. Mitochondria are the cell organelle most susceptible to aggression. We observed a moderate tendency toward a decreased efficiency of mitochondrial oxidative phosphorylation coupling in the PMV group, probably by generating an unstable energized state in the cristae membrane. After PMV such muscle damage probably contributes in parts to difficulties in weaning the patients.

**Acknowledgements** This work was carried out in collaboration with the Centre Regional d'Imagerie Cellulaire Montpellier, France. The results were presented in part at the American Thoracic Society meeting, San Diego, California, 23–28 April 1999 and at the Société de Réanimation de Langue Française meeting, Paris, France, 19–22 January 1999.

## References

1. Slutsky AZ (1994) Consensus conference on mechanical ventilation. January 28–30, 1993 at Northbrook, Illinois USA. II. Intensive Care Med 20:150–162
2. Brochard L, Harf A, Lorino H, Lemaire F (1989) Inspiratory pressure support prevents diaphragmatic fatigue during weaning from mechanical ventilation. Am Rev Respir Dis 139:513–521
3. Lemaire F (1993) Difficult weaning. Intensive Care Med 19:S69–S73
4. MacIntyre NR (1997) Ventilatory muscles and mechanical ventilatory support. Crit Care Med 25:1106–1107
5. Mancebo J (1996) Weaning from mechanical ventilation. Eur Respir J 9:1923–1931
6. Tobin MJ (1996) Role of the respiratory muscle during weaning from mechanical ventilation. Reanimation Soins Intensifs Med Urgence 5:719–724
7. Desplanches D, Kayar SR, Sempore B, Flandrois R, Hoppeler H (1990) Rat soleus muscle ultrastructure after hindlimb suspension. J Appl Physiol 69:504–508
8. Booth FW (1982) Effect of limb immobilization on skeletal muscle. J Appl Physiol 52:1113–1118
9. Witzmann FA, Kim DH, Fitts RH (1983) Effects of hindlimb immobilization on the fatigability of skeletal muscle. J Appl Physiol 54:1242–1248
10. Joffe M, Savage N, Isaacs H (1983) Respiratory activities of subsarcolemmal and intermyofibrillar mitochondrial populations isolated from denervated and control rat soleus muscles. Comp Biochem Physiol B Biochem Mol Biol 76:783–787
11. Krieger DA, Tate CA, McMillin-Wood J, Booth FW (1980) Populations of rat skeletal muscle mitochondria after exercise and immobilization. J Appl Physiol 48:23–28
12. Max SR (1972) Disuse atrophy of skeletal muscle: loss of functional activity of mitochondria. Biochem Biophys Res Commun 46:1394–1398
13. Yajid F, Mercier JG, Mercier BM, Dubouchaud H, Préfaut C (1998) Effects of 4 weeks of hindlimb suspension on skeletal muscle mitochondrial respiration in rats. J Appl Physiol 84:479–485
14. Kauhanen S, Leivo I, Michelsson JE (1993) Early muscle changes after immobilization. Clin Orthop 297:44–50
15. Leivo I, Kauhanen S, Michelsson JE (1998) Abnormal mitochondrial and sarcoplasmic changes in rabbit skeletal muscles induced by immobilization. APMIS 106:1113–1123
16. McGeachi JK (1989) Sustained cell proliferation in denervated skeletal muscle of mice. Cell Tissue Res 257:455–457
17. Sieck GC (1994) Physiological effects of diaphragm muscle denervation and disuse. Clin Chest Med 15:641–659
18. Yellin H (1974) Changes in fiber types of the hypertrophying denervated hemidiaphragm. Exp Neurol 42:412–428
19. Zhan W-Z, Sieck GC (1992) Adaptations of diaphragm and medial gastrocnemius muscles to inactivity. J Appl Physiol 72:1445–1453
20. Zhan W-Z, Farkas GA, Schroeder MA, Gosselin LE, Sieck GC (1995) Regional adaptations of rabbit diaphragm muscle fibers to unilateral denervation. J Appl Physiol 79:941–950
21. Gosselin LE, Brice G, Carlson B, Prakash YS, Sieck GC (1994) Changes in satellite cell mitotic activity during acute period of unilateral diaphragm denervation. J Appl Physiol 77:1128–1134
22. Le Bourdelles G, Viires N, Boczkowski J, Seta N, Pavlovic D, Aubier M (1994) Effects of mechanical ventilation on diaphragmatic contractile properties in rats. Am J Respir Crit Care Med 149:1539–1544
23. Anzueto A, Peters JI, Tobin MJ, De Los Santos R, Seidenfeld JJ, Moore G, Cox WJ, Coalson JJ (1997) Effects of prolonged controlled mechanical ventilation on diaphragmatic function in healthy adult baboons. Crit Care Med 25:1187–1190
24. Yang L, Luo J, Lin M-C, Gottfried SB, Petrof BJ (1997) Effects of long-term mechanical ventilation on rat diaphragm mass and myosin heavy chain expression. Am Rev Respir Crit Care Med A509
25. Davies KJA, Packer L, Brooks G (1981) Biochemical adaptation of mitochondria, muscle, whole animal respiration to endurance training. Arch Biochem Biophys 209:539–554
26. Bernardi P, Petronilli V, Di Lisa F, Forte M (2001) A mitochondrial perspective on cell death. Trends Biochem Sci 26:112–117
27. Flecknell PA (1993) Anaesthesia of animals for biomedical research. Br J Anaesth 71:885–894
28. Bradford M (1976) A rapid sensitive method for the quantification of microgram quantities of protein utilizing the principle of protein-dye binding. Anal Biochem 72:248–254

29. Estabrook RW (1967) Mitochondrial respiratory control and the polarographic measurement of ADP:O ratios. Methods Enzymol 10:41–7
30. Anzil AP, Sancesario G, Massa R, Bernardi G (1991) Myofibrillar disruption in the rabbit soleus muscle after one-week hindlimb suspension. Muscle Nerve 14:358–369
31. Appell HJ (1986) Morphology of immobilized skeletal muscle and the effect of a pre- and postimmobilization training program. Int J Sports Med 7:6–12
32. Cooper RR (1972) Alterations during immobilization and regeneration of skeletal muscle in cats. J Bone Joint Surg Am 54:919–953
33. Tomanek RJ, Lund DD (1974) Degeneration of different types of skeletal muscle fibers Immobilization. J Anat 118:531–541
34. Miledi R, Slater C (1968) Some mitochondrial changes in denervated muscle. J Cell Sci 3:49–54
35. Muscatello U, Margreth A, Aloisi M (1965) On the differential response of sarcoplasm and myoplasm to denervation in frog muscle. J Cell Biol 27:1–24
36. Willis WT, Jackman MR (1994) Mitochondrial function during heavy exercise. Med Sci Sports Exerc 26:1347–1354
37. Brody TM, Bain JA (1954) Barbiturates and oxydative-phosphorylation. J Pharmacol Exp Ther 110:148–156
38. Chance B, Hollunger G (1963) Inhibition of electron and energy transfer in mitochondria. 1. Effects of amytal, thiopental, rotenone, progesterone, and methylene glycol. J Biol Chem 278:418–431
39. Cohen PJ (1973) Effect of anesthetics on mitochondrial function. Anesthesiology 39:153–164
40. Nahrwold ML, Cohen PJ (1975) Anesthetics and mitochondrial respiration. Clin Anesth 11:25–44
41. Aldridge WN, Parker VH (1960) Barbiturates and oxidative phosphorylation. Biochem J 76:47–56
42. Benzi G, Agnoli A, Dagani F, Ruggieri S, Villa RF (1979) Effect of phenobarbital on cerebral energy state and metabolism. Enzymatic activities. Stroke 10:733–735
43. Takaki M, Nakahara H, Kawatani Y, Utsumi K, Hiroyuki S (1997) No suppression of respiratory function of mitochondria isolated from the hearts of anesthetized rats with high-dose Pentobarbital Sodium. Jpn J Physiol 47:87–92
44. Cabanne F, Bonenfant JL (1986) Anatomie pathologique. Principe de pathologie générale, de pathologie spéciale et d'ætopathologie, 2nd edn. Maloine, Paris, pp 9–53
45. Jolly W, Harris RA, Asai J, Lenaz G, Green DE (1969) Studies on ultrastructural dislocations in mitochondria. II. On the dislocation induced by lyophilization and the mechanism of uncoupling. Arch Biochem Biophys 130:191–211